



Cite this: *Chem. Commun.*, 2015, 51, 4001

Received 24th December 2014,  
Accepted 19th January 2015

DOI: 10.1039/c4cc10304a

www.rsc.org/chemcomm

## Photocontrolled chignolin-derived $\beta$ -hairpin peptidomimetics†

T. Podewin,<sup>a</sup> M. S. Rampp,<sup>b</sup> I. Turkanovic,<sup>b</sup> K. L. Karaghiosoff,<sup>a</sup> W. Zinth<sup>\*b</sup> and A. Hoffmann-Röder<sup>\*a</sup>

The synthesis of novel, chignolin-derived peptides comprising the azobenzene photoswitch [3-(3-aminomethyl)phenylazo]phenylacetic acid (AMPP) is reported. Reversible photoswitching behavior led to folding into  $\beta$ -hairpin-like structures, as unequivocally demonstrated by CD, FT-IR and NMR spectroscopy.

Understanding the mechanisms, by which particular sequences of amino acids are folded into well-defined three-dimensional protein structures, is a challenging problem in the field of molecular biology. The complexity of possible conformational transitions and different timescales of folding prevents accurate predictions and simulations for larger amino acid ensembles. Moreover, it is believed that certain key secondary motifs, *e.g.*  $\beta$ -hairpins and  $\beta$ -sheets, serve as nucleation sites for protein folding, providing insight into the early events of secondary structure formation. In particular  $\beta$ -hairpin-forming peptides have received much attention as model systems for both experimental and theoretical studies of the initial folding steps.<sup>1–4</sup> For instance, light-triggered folding of two amino acids strands into a  $\beta$ -hairpin peptide has been investigated by means of azobenzene photoswitches,<sup>5–10</sup> such as [3-(3-aminomethyl)phenylazo]phenylacetic acid<sup>11–13</sup> (AMPP). Upon incorporation into the peptide backbone, the latter offers the possibility to control the hairpin structure by initiating a reversible folding (*cis*-form) or unfolding (*trans*-form) transition.

Herein, we present a peptidomimetic model system for photocontrolled reversible  $\beta$ -hairpin formation based on chignolin<sup>14</sup> and AMPP. The decapeptide chignolin (GYDPETGTWG) was designed by Honda *et al.* on the basis of the central part of the GB1 hairpin<sup>14–17</sup> and is the smallest  $\beta$ -hairpin known to be stable in solution. As such

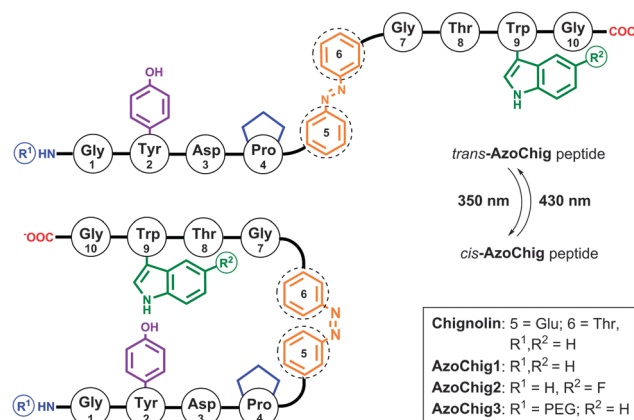


Fig. 1 Representative schematic illustration of reversible *cis*  $\rightleftharpoons$  *trans* isomerization of **AzoChig** peptides at 350 and 430 nm, respectively.

and in combination with ultrafast initiation of structural changes upon photoswitching, chignolin derivatives are particularly attractive targets for folding studies of protein nuclei. Therefore, the peptide **AzoChig1** (GYDP-AMPP-GTWG) was designed, in which the two central amino acids Glu5 and Thr6 of chignolin's four-residue turn sequence were substituted by AMPP (Fig. 1). Besides, peptidomimetic **AzoChig2** (GYDP-AMPP-GT(5FW)G) with a 5-fluoro-*l*-tryptophan (5FTrp, 5FW) residue instead of Trp9 was synthesized to enhance key hydrophobic interactions between aromatic Tyr2 and Trp9. Fluorinated amino acid residues are known to be tolerated by a variety of proteins without introducing much steric perturbation and usually favor protein folding and stability due to their increased hydrophobicity.<sup>18,19</sup> For instance, the hydrophobicity of 5FTrp, derived from 1-octanol–water partitioning experiments, is significantly higher than that of native Trp.<sup>20,21</sup> However, systematic studies towards structure-guiding effects of fluorinated amino acids have mostly focused on  $\alpha$ -helical systems<sup>19,22</sup> and only a limited number of approaches for fluorination of specific  $\beta$ -sheet positions have been reported, so far.<sup>23</sup> Finally, since both peptides **AzoChig1** and **AzoChig2** showed high solubility only in polar solvents like MeOH and MeCN, **AzoChig3** ((TEG)GYDP-AMPP-GTWG), equipped

<sup>a</sup> Department of Organic Chemistry, Faculty of Chemistry and Pharmacy, Ludwig-Maximilians-University LMU, 81377 Munich, Germany. E-mail: anja.hoffmann-roeder@cup.lmu.de

<sup>b</sup> Department for BioMolecular Optics, Faculty of Physics, Ludwig-Maximilians-University LMU, 80538 Munich, Germany. E-mail: wolfgang.zinth@physik.uni-muenchen.de

† Electronic supplementary information (ESI) available: Experimental procedures, analytical data and selected spectra of all new compounds. See DOI: 10.1039/c4cc10304a



with an additional, N-terminal triethylene glycol residue, was prepared to furnish a photoswitchable and water-soluble chignolin derivative. Key amino acid building blocks for the solid-phase peptide synthesis (SPPS) of photocontrolled chignolin-derived  $\beta$ -hairpins were prepared, as follows (ESI<sup>†</sup>): Fmoc-protected AMPP derivative was synthesized in seven steps according to the known strategy of Renner *et al.*<sup>12</sup> Thus, (9H-fluoren-9-yl)methyl-(3-aminobenzyl)carbamate, derived from Fmoc-protection of 3-(aminomethyl)aniline, was reacted with 2-(3-nitrosophenyl)acetic acid under Mills conditions to afford the AMPP building block in 59% yield.

Fmoc-protection of commercially available 5FTrp yielded the requisite fluorinated building block, while the Fmoc-TEG derivative was synthesized in five steps starting from triethylene glycol.<sup>24</sup> The chignolin-derived peptides were assembled in an automated microwave-assisted CEM Liberty 1 peptide synthesizer on a pre-loaded Fmoc-Gly-Wang LL resin (Novabiochem).

After Fmoc-deprotection by piperidine in *N*-methylpyrrolidone (NMP), the standard amino acid couplings were performed using HBTU-HOBt and diisopropylethylamine in DMF for activation. In contrast, incorporation of the non-standard building blocks required modified coupling procedures and the use of the more

reactive HATU-HOAt-*N*-methylmorpholine cocktail. Release from the resin with simultaneous deprotection using TFA-H<sub>2</sub>O mixtures (95:5) followed by preparative RP-HPLC, finally provided the targeted chignolin-derived peptidomimetics with yields of 10–33%.

Photomodulation of  $\beta$ -hairpins with azobenzene derivatives as backbone elements mostly relies on an ultrafast *trans*  $\leftrightarrow$  *cis* isomerization, which can be induced by light of different wavelengths and involves large changes in geometry and dipole moments.<sup>25,26</sup> For instance, *cis*-AMPP-TrpZip peptides forming a  $\beta$ -hairpin-like structure can rapidly unfold within 1 ns by photoisomerization of AMPP to its *trans*-isomeric state.<sup>12,27,28</sup> In chignolin, the  $\beta$ -hairpin conformation is stabilized by H bonds of Asp3:N-Thr8:O, Gly7:N-Asp3:O<sup>δ</sup>, Thr8:N-Asp3:O, Glu5:N-Asp3:O<sup>δ</sup> and Thr6:N-Asp3:O<sup>δ</sup>, as well as by hydrophobic interactions between Tyr2:Pro4 and Tyr2:Trp9.<sup>29</sup> The newly synthesized **AzoChig** derivatives should retain most of the aforementioned stabilizing interactions, and in particular **AzoChig2** comprising the 5FTrp residue should reveal enhanced hydrophobic interactions between Tyr2 and Trp9 (*vide supra*).

RP-HPLC analyses and NMR spectroscopy demonstrate the structural integrity and purity of the assembled **AzoChig1–3**

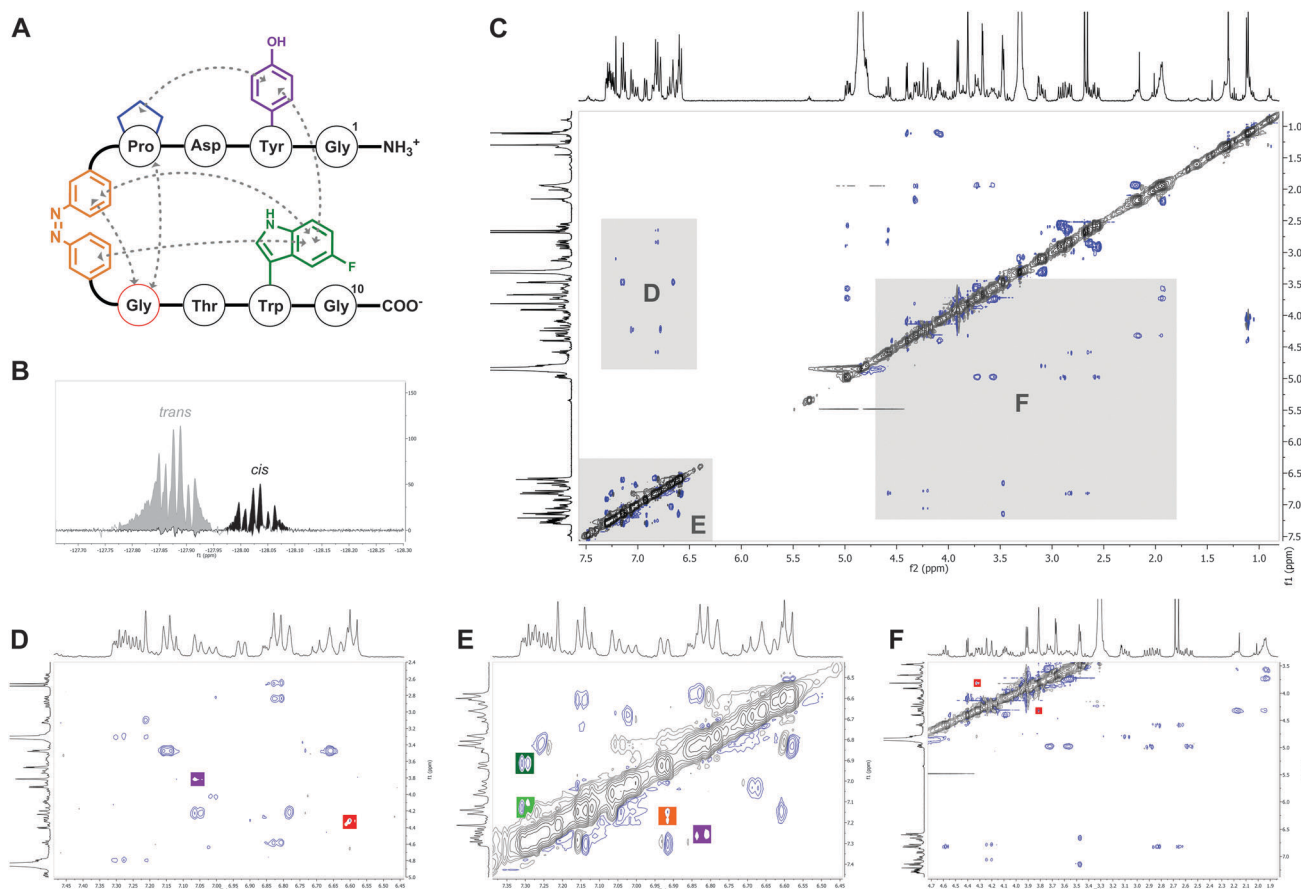


**Fig. 2** (A) Schematic structure of *cis*-**AzoChig2** with observed NOE cross peaks (gray) between Tyr2, Pro4, AMPP5,6 and Trp9; (B) <sup>19</sup>F-NMR spectra of *cis*- (black) and *trans*-**AzoChig2** (grey) peptides in MeOH-*d*<sub>4</sub> at 26 °C, *c* = 2 mM; (C) <sup>1</sup>H,<sup>1</sup>H-ROESY-NMR spectra of **AzoChig2** in MeOH-*d*<sub>4</sub> at 26 °C, *c* = 2 mM; (D) <sup>1</sup>H,<sup>1</sup>H-ROESY-NMR section from 7.5–6.5 and 5.0–2.4 ppm. Marked NOE cross peaks: Tyr2/H3,H5  $\leftrightarrow$  Pro4/H $\alpha$  (red) and AMPP5,6/H8  $\leftrightarrow$  Gly7/H $\alpha$ ,H $\alpha'$  (purple); (E) <sup>1</sup>H,<sup>1</sup>H-ROESY-NMR section from 7.4–6.4 and 7.4–6.5 ppm. Marked NOE cross peaks: Tyr2/H2,H6  $\leftrightarrow$  Trp9/H6 (purple), AMPP5,6/H7  $\leftrightarrow$  AMPP5,6/H16 (orange), AMPP5,6/H7  $\leftrightarrow$  Trp9/H4 (dark green) and AMPP5,6/H16  $\leftrightarrow$  Trp9/H4 (green); (F) <sup>1</sup>H,<sup>1</sup>H-ROESY-NMR section from 4.7–1.9 and 7.5–3.5 ppm. Marked NOE cross peaks: Pro4/H $\alpha$   $\leftrightarrow$  Gly7/H $\alpha$ ,H $\alpha'$  (red).



mimetics (ESI<sup>†</sup>). To elucidate the three-dimensional solution structures of *cis*-/*trans*-**AzoChig1–3**, <sup>1</sup>H and <sup>13</sup>C, as well as correlation (COSY), hetero nuclear single quantum (HSQC) and hetero nuclear multiple bond (HMBC) NMR spectra were recorded in 10 mM MeOH-*d*<sub>4</sub> solutions at 400 and 600 MHz.<sup>30</sup> Unfortunately though, **AzoChig3** aggregates strongly in solution, which leads to heavy signal broadening and precludes any precise signal assignments. In contrast, sharp <sup>1</sup>H NMR signals, unequivocally assignable were obtained for *cis*-/*trans*-**AzoChig1** and **2**, enabling their application to total correlation (TOCSY) and rotating-frame nuclear Overhauser enhancement (ROESY) spectroscopy at 400 MHz in MeOH-*d*<sub>4</sub> (Fig. 2C–F). All samples were kept in the dark for two days before measurement, yielding *trans*-configured peptides.

The <sup>1</sup>H NMR spectra of **AzoChig1** and **AzoChig2** peptides show distinct peak offsets for the aromatic residues Tyr2, AMPP5,6 and Trp9 (8.0–6.5 ppm) upon *cis* ⇌ *trans* isomerizations. Moreover, NOE cross-peaks detected between Tyr2:Trp9, Pro4:Gly7, AMPP5,6:Gly7 and AMPP5,6:Trp9 in the ROESY spectra of *cis*-**AzoChig1** and *cis*-**AzoChig2**, depict the expected formation of folded structures for both derivatives (Fig. 2D–F), with NOE signals between aromatic Tyr2, AMPP5,6 and Trp9 moiety, pinpointing the presence of turns stabilized by hydrophobic interactions. The <sup>19</sup>F NMR spectra of *cis*- and *trans*-**AzoChig2** finally reveal distinct downfield shifts of the fluorine signals (Fig. 2B), indicating significant changes in the electronic structure and interactions upon isomerization.

To substantiate the presence of unfolded *trans*-conformations and their conversions into the desired β-hairpin structures upon azobenzene *trans*-to-*cis* isomerizations, UV/Vis, FT-IR, and CD spectroscopic measurements were performed. Therefore, 1 mM stock solutions of **AzoChig1–3** peptides in MeOH were prepared and stored in the dark at room temperature for two days,

furnishing *trans*-configured peptides. Using these stock solutions, peptide samples with concentrations of *c* = 76 μM (**AzoChig1**), 77 μM (**AzoChig2**) and 78 μM (**AzoChig3**) were prepared through dilution with MeOH to record stationary UV/Vis absorption spectra before and after illumination at appropriate wavelengths (Fig. 3A). Irradiation of the *trans*-peptides at λ = 350 nm for 180 s led to reversible formation of photostationary states comprising in each case 84% of the *cis*-conformer. The UV spectra of *trans*-**AzoChig1** and *trans*-**AzoChig3** are very similar and show characteristic maxima at 322 nm and 291 nm due to the π → π\* *trans*-azobenzene transition and the absorptions by Trp9 and Tyr2. The latter maximum is shifted towards 299 nm in the **AzoChig2** spectrum as a result of the presence of the 5FTrp moiety.

Stationary FT-IR spectra of the *trans*-**AzoChig** peptides were recorded using 5 mM solutions in MeOH-*d*<sub>4</sub>, which were kept again in the dark for two days. MeOH-H<sub>2</sub>O mixtures were spared to avoid the undesired aggregation of the peptidomimetics. The spectra of all peptides are similar featuring the characteristic bands of the azobenzene chromophore and the peptide backbones (amide I and II bands around 1655 cm<sup>-1</sup> and 1450 cm<sup>-1</sup>, respectively, Fig. 3B). The peak at 1675 cm<sup>-1</sup> originates from traces of TFA used during preparation of the samples. The difference spectra were recorded for *trans* → *cis* and *cis* → *trans* isomerizations (Fig. 3C). Most prominent in the difference spectra is the dispersive line shape in the range of the amide I band, which points to a change in the H-bonding pattern upon isomerization of the azobenzene. In the *cis*-isoform there is an excess of strong H bonds, red-shifted relative to weaker H bonds, which were found preferentially in the *trans*-form of the peptides. This feature, similar to the one observed previously in ATZ,<sup>12,27,28</sup> points to a change of the peptide structure with an open *trans*-form to a compact *cis*-form. Latter thereby shows

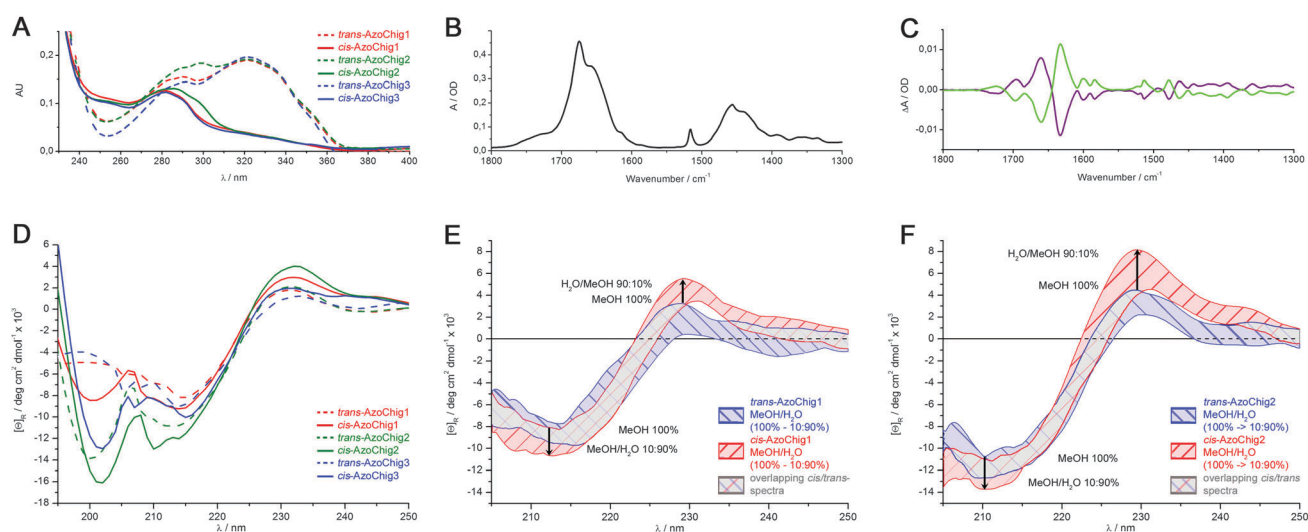


**Fig. 3** (A) UV/Vis spectra of *cis*-/*trans*-**AzoChig1–3** at 25 °C, *c* = 76–78 μM; (B) representative FT-IR absorption spectrum of **AzoChig1** at 25 °C in MeOH-*d*<sub>4</sub>, *c* = 5 mM; (C) absorption difference spectra of **AzoChig1** induced by irradiations at 350 nm (*trans* → *cis*, green curve) and 430 nm (*cis* → *trans*, purple curve) in MeOH-*d*<sub>4</sub>, *c* = 5 mM; (D) CD spectra of *cis*-/*trans*-**AzoChig1–3** at 5 °C in MeOH, *c* = 76–78 μM; (E) solvent-dependent CD spectra of *cis*-**AzoChig1** (red hatched band) and *trans*-**AzoChig1** (blue hatched band) at 5 °C in MeOH-H<sub>2</sub>O ratios reaching from 100% MeOH → MeOH-H<sub>2</sub>O 10/90 with *c* = 82–112 μM. The gray crossed band represents overlapping spectra; (F) solvent-dependent CD spectra of *cis*-**AzoChig2** (red hatched band) and *trans*-**AzoChig2** (blue hatched band) at 5 °C in MeOH-H<sub>2</sub>O ratios reaching from 100% MeOH → MeOH-H<sub>2</sub>O 10/90 with *c* = 84–102 μM. The gray crossed band represents overlapping spectra.



additional stronger, presumably interstrand H bonds pointing to a  $\beta$ -hairpin-like structure.

CD spectra in the 195–250 nm range were determined for *trans*-**AzoChig1–3** peptides at concentrations of  $c = 76\text{--}78\ \mu\text{M}$  in MeOH at  $5\ ^\circ\text{C}$  (*vide supra*). Solvent-dependent CD spectra of **AzoChig1** and **AzoChig2** were recorded at concentrations of  $c = 82\text{--}112\ \mu\text{M}$  in MeOH–H<sub>2</sub>O mixtures at  $5\ ^\circ\text{C}$ . For the *cis*-azo isomers, CD spectra were recorded after irradiation at 350 nm for 180 s, *i.e.*, at the *cis*-photostationary state (Fig. 3D). All three *cis*-azo peptides feature distinct maxima at 231 nm – assigned to stacking of Trp9 to Tyr2 – as well as minima at 212 nm and 200 nm, and pronounced positive signals below 195 nm. Hence, they strongly resemble the spectra of native chignolin suggesting a folded, hairpin-like structure. The enhanced hydrophobic interactions between Tyr2 and 5FTrp9 in **AzoChig2** become visible by the increase of the CD signal in the 231 nm range. Temperature-dependent CD spectra of *cis*-**AzoChig1** and *cis*-**AzoChig2** in the 5–60  $^\circ\text{C}$  range (data not shown, see ESI<sup>†</sup>) reveal a thermal unfolding process to be working at higher temperatures, similar to native chignolin. The CD spectra of *trans*-**AzoChig1–3** display small maxima at 231 nm and minima at 213 nm but deviate in the 200 nm range. The deep minimum found for **AzoChig2** at 200 nm can be tentatively interpreted in terms of a better ordering of the peptide part due to the increased hydrophobic interaction of 5FTrp9 with Tyr2.

Moreover, solvent-dependent CD measurements were performed using mixtures of MeOH–H<sub>2</sub>O (Fig. 3E and F, see ESI<sup>†</sup>), with ratios from 10–100% MeOH. The MeOH–H<sub>2</sub>O spectra of the *cis*-/*trans*-**AzoChig1** and *cis*-/*trans*-**AzoChig2** peptidomimetics show increasing values for the maximum around 230 nm and deeper minima at 200 nm with increasing water amounts. Presumably, the hydrophobic turn region of the *cis*-peptides becomes more stabilized by hydrophobic interactions between Tyr2:Trp9 in aqueous surroundings, which leads to the observed increase in molar ellipticity at 230 nm. Furthermore, interstrand interactions are stabilized by water-mediated hydrogen bonding as reflected by the decreased ellipticity around 200 nm. Finally and at higher water ratios, the observed CD signals of **AzoChig1** and **AzoChig2** approximate nicely the reported molar ellipticity characteristics of the parent peptide chignolin.<sup>14</sup>

We have presented a novel class of photoswitchable  $\beta$ -hairpin model peptides derived from the designer mini protein chignolin by substitution of two central amino acids from the turn sequence by the known azobenzene chromophore AMPP. The resulting **AzoChig1–3** peptidomimetics were assembled by SPPS and carefully characterized at both photoisomeric states using UV/VIS, IR, CD, and NMR spectroscopy. In the *trans*-state of AMPP, the peptides mostly exhibit a disordered structure, while *trans*  $\rightarrow$  *cis* photoisomerization of the azobenzene chromophore induces folded  $\beta$ -hairpin-like structures.

Support from LMU Munich, the Deutsche Forschungsgemeinschaft (SFB 749, project A5) and the Excellence Cluster CIPSM – Center of Integrated Protein Science Munich – is gratefully acknowledged.

## Notes and references

- 1 C. E. Stotz and E. M. Topp, *J. Pharm. Sci.*, 2004, **93**, 2881–2894.
- 2 A. G. Cochran, N. J. Skelton and M. A. Starovasnik, *Proc. Natl. Acad. Sci. U. S. A.*, 2001, **98**, 5578–5583.
- 3 A. Lewandowska, S. Oldziej, A. Liwo and H. A. Scheraga, *Biophys. Chem.*, 2010, **151**, 1–9.
- 4 K. Lindorff-Larsen, S. Piana, R. O. Dror and D. E. Shaw, *Science*, 2011, **334**, 517–520.
- 5 S. Samanta, A. A. Beharry, O. Sadovski, T. M. McCormick, A. Babalhavaej, V. Tropepe and G. A. Woolley, *J. Am. Chem. Soc.*, 2013, **135**, 9777–9784.
- 6 A. M. Ali and G. A. Woolley, *Org. Biomol. Chem.*, 2013, **11**, 5325–5331.
- 7 F. Zhang, K. M. Mueller, G. A. Woolley and K. M. Arndt, *Methods Mol. Biol.*, 2012, **813**, 195–210.
- 8 M. Blanco-Lomas, S. Samanta, P. J. Campos, G. A. Woolley and D. Sampedro, *J. Am. Chem. Soc.*, 2012, **134**, 6960–6963.
- 9 A. A. Beharry, T. Chen, M. S. Al-Abdul-Wahid, S. Samanta, K. Davidov, O. Sadovski, A. M. Ali, S. B. Chen, R. S. Prosser, H. S. Chan and G. A. Woolley, *Biochemistry*, 2012, **51**, 6421–6431.
- 10 O. Sadovski, A. A. Beharry, F. Zhang and G. A. Woolley, *Angew. Chem., Int. Ed.*, 2009, **48**, 1484–1486.
- 11 A. A. Beharry and G. A. Woolley, *Chem. Soc. Rev.*, 2011, **40**, 4422–4437.
- 12 S.-L. Dong, M. Löweneck, T. E. Schrader, W. J. Schreier, W. Zinth, L. Moroder and C. Renner, *Chem. – Eur. J.*, 2006, **12**, 1114–1120.
- 13 A. Aemissegger, V. Kräutler, W. F. van Gunsteren and D. Hilvert, *J. Am. Chem. Soc.*, 2005, **127**, 2929–2936.
- 14 S. Honda, K. Yamasaki, Y. Sawada and H. Morii, *Structure*, 2004, **12**, 1507–1518.
- 15 M. Bonomi, D. Branduardi, F. L. Gervasio and M. Parrinello, *J. Am. Chem. Soc.*, 2008, **130**, 13938–13944.
- 16 B. Ma and R. Nussinov, *J. Mol. Biol.*, 2000, **296**, 1091–1104.
- 17 S. Honda, T. Akiba, Y. S. Kato, Y. Sawada, M. Sekijima, M. Ishimura, A. Oishi, H. Watanabe, T. Odahara and K. Harata, *J. Am. Chem. Soc.*, 2008, **130**, 15327–15331.
- 18 B. C. Buer, J. L. Meagher, J. A. Stuckey and E. N. G. Marsh, *Proc. Natl. Acad. Sci. U. S. A.*, 2012, **109**, 4810–4815.
- 19 M. Salwiczek, E. K. Nyakatura, U. I. M. Gerling, S. Ye and B. Kokschi, *Chem. Soc. Rev.*, 2012, **41**, 2135–2171.
- 20 Z. J. Xu, M. L. Love, L. Y. Ma, M. Blum, P. M. Bronskill, J. Bernstein, A. A. Grey, T. Hofmann, N. Camerman and J. T. Wong, *J. Biol. Chem.*, 1989, **264**, 4304–4311.
- 21 C.-Y. Wong and M. R. Eftink, *Biochemistry*, 1998, **37**, 8947–8953.
- 22 C. J. Pace and J. Gao, *Acc. Chem. Res.*, 2012, **46**, 907–915.
- 23 G. A. Clark, J. D. Baleja and K. Kumar, *J. Am. Chem. Soc.*, 2012, **134**, 17912–17921.
- 24 S. Keil, C. Claus, W. Dippold and H. Kunz, *Angew. Chem., Int. Ed.*, 2001, **40**, 366–369.
- 25 H. Fliegl, A. Köhn, C. Hättig and R. Ahlrichs, *J. Am. Chem. Soc.*, 2003, **125**, 9821–9827.
- 26 J. Dokić, M. Gothe, J. Wirth, M. V. Peters, J. Schwarz, S. Hecht and P. Saalfrank, *J. Phys. Chem.*, 2009, **113**, 6763–6773.
- 27 A. A. Deeg, M. S. Rampp, A. Popp, B. M. Pilles, T. E. Schrader, L. Moroder, K. Hauser and W. Zinth, *Chem. – Eur. J.*, 2014, **20**, 694–703.
- 28 T. E. Schrader, W. J. Schreier, T. Cordes, F. O. Koller, G. Babitzki, R. Denschlag, C. Renner, M. Löweneck, S.-L. Dong, L. Moroder, P. Tavan and W. Zinth, *Proc. Natl. Acad. Sci. U. S. A.*, 2007, **104**, 15729–15734.
- 29 S. Enemark and R. Rajagopalan, *Phys. Chem. Chem. Phys.*, 2012, **14**, 12442–12450.
- 30 In consequence of the limited solubility of peptidomimetics **AzoChig1** and **AzoChig2** in aqueous solutions and their intrinsic aggregation tendency at very high concentrations (> 5 mM), spectroscopic conformational analyses were performed in MeOH, similar to related model studies (see *e.g.* ref. 12 and 28 and following references: (a) M. Erdélyi, A. Karlén and A. Gogoll, *Chem. – Eur. J.*, 2006, **12**, 403–412; (b) M. Erdélyi, V. Langer, A. Karlén and A. Gogoll, *New J. Chem.*, 2002, **26**, 834–843; (c) Y. J. Chung, B. R. Huck, L. A. Christianson, H. E. Stanger, S. Kräuthauser, D. R. Powell and S. H. Gellman, *J. Am. Chem. Soc.*, 2000, **122**, 3995–4004). Finally, it must be emphasized that so far, the **AzoChig** peptides represent first model compounds and will be further optimized for folding studies under more physiological conditions. These optimizations require greater divergence from the original chignolin design and are subject to extended future studies.

